Biophoton detection as a novel technique for cancer imaging

Motohiro Takeda,[1] Masaki Kobayashi,[2] Mariko Takayama,[3] Satoshi Suzuki,[2] Takanori Ishida,[1] Kohji Ohnuki,[1] Takuya Moriya[4] and Noriaki Ohuchi[1, 5]

[1]Division of Surgical Oncology, [3]Division of Dermatology and [4]Division of Pathology, Tohoku University Graduate School of Medicine, 1-1 Seiryo-machi, Aoba-ku, Sendai 980-8574; and [2]Division of Electronics, Tohoku Institute of Technology, 35 Kasumi-cho, Yagiyama, Taihaku-ku, Sendai 982-8577

(Received February 16, 2004/Revised June 16, 2004/Accepted June 16, 2004)

Biophoton emission is defined as extremely weak light that is radiated from any living system due to its metabolic activities, without excitation or enhancement. We measured biophoton images of tumors transplanted in mice with a highly sensitive and ultra-low noise CCD camera system. Cell lines employed for this study were AH109A, TE4 and TE9. Biophoton images of each tumor were measured 1 week after carcinoma cell transplantation to estimate the tumor size at week 1 and the biophoton intensity. Some were also measured at 2 and 3 weeks to compare the biophoton distribution with histological findings. We achieved sequential biophoton imaging during tumor growth for the first time. Comparison of microscopic findings and biophoton intensity suggested that the intensity of biophoton emission reflects the viability of the tumor tissue. The size at week 1 differed between cell lines, and the biophoton intensity of the tumor was correlated with the tumor size at week 1 (correlation coefficient 0.73). This non-invasive and simple technique has the potential to be used as an optical biopsy to detect tumor viability. (Cancer Sci 2004; 95: 656–661)

Ultraweak biophoton emission is defined as extremely weak light originating from living things as a result of their metabolic activities. This phenomenon has been recognized to occur without enhancement or excitement by chemical administration or light irradiation. Ultraweak biophoton emission ranges from the ultraviolet to the near infrared, and its intensity is generally lower than 10^{-9} W/cm^2, i.e., less than 1/1000 of the human visible light intensity.

Many living systems have been shown to exhibit biophoton emission since the invention of photo-multiplier tubes,[1)] including proliferating *Saccharomyces cerevisiae*, longitudinal sections of bamboo shoot, injured soybean seedlings and fertilizing sea urchins.[2–5)] All the results are consistent with pathological or physiological significance of biophoton emission. Samples from human beings, including smoker's breath and serum, also exhibit ultraweak light emission.[6)] Thus, biophoton emission may be an indicator of pathological conditions in patients.

Cancer is a major cause of human mortality, and many diagnostic methods have been developed. Trials on ultraweak biophoton measurement of the serum or urine from cancer patients have also been performed for diagnostic applications.[7, 8)] Elevation of ultraweak light intensity from serum or urine has been attributed to metabolic changes in patients. Thus, measurement of carcinoma lesions might provide more accurate information on the pathological status of cancer. Shimizu *et al*. measured biophoton intensity from transplanted malignant tumors[9)] and observed differences among the tumors, and Amano *et al*. presented biophoton images of bladder cancer transplanted in nude mice.[10)] Although these results suggest the feasibility of biophoton measurement for cancer diagnosis, there has been no report discussing applications based on specific pathological features for cancer diagnosis.

In a recent study, we detected changes in biophoton emission from proliferating carcinoma cell cultures using a flow culture system coupled with a highly sensitive apparatus.[11)] In the present study, TE9, an esophageal carcinoma cell line, exhibited quite similar changes in biophoton intensity during cell proliferation, and we measured the specific biophoton spectrum of a cell culture for the first time. The results demonstrated the applicability of biophoton measurement to the detection of cell proliferation for cancer diagnosis. Growth rate is one of the most important of the factors that define malignancy, and the results lead to the idea that biophoton emission may reflect the growth potential of the tumor.

In the present study, we investigated the relationship between biophoton intensity and tumor size after 1 week to ascertain the relationship of biophoton properties with the tumor growth potential. Furthermore, we took weekly measurements of the biophoton images of 3 different types of tumor for 2 or 3 weeks and compared them with the tumor histology to clarify the relationship between tissue distribution and the two-dimensional biophoton emission image. The feasibility of specific application of biophoton imaging is discussed.

Materials and Methods

Instrumentation. For the imaging of ultraweak light emission, a cooled charge-coupled device (CCD) camera system (ATC200C, Photometrics, Inc.) was utilized. A back-illuminated type of CCD (TK1024AB2, Tektronix, Inc.) is incorporated in the camera system with cooling at –120°C using liquid nitrogen. The camera head is mounted on a completely light-tight chamber, which includes a temperature-controlled mounting bed to maintain the body temperature of a mouse (Fig. 1).[12)] A lens system (Nikor F/1.2, Nikon) was used for imaging an observation area measuring 100×100 mm. The CCD has a spectral sensitivity over the wavelength range from 400 to 1000 nm with a maximum quantum efficiency of 73% at 700 nm. Pixel size of the CCD is 24×24 μm with 1024×1024 format. In the experiments, the CCD camera was operated in 2×2 binning mode, with a resulting spatial resolution of 48×48 μm, which corresponded to a resolution of 190 μm on the object. Integration time for each measurement was 1 h. The minimum detectable intensity of the emission on a sample surface under the above condition is estimated to be 1.0×10^4 photons/s/cm^2, taking into account read-out noise and the dark current of the CCD, and the total light detection efficiency of the system. One count of the intensity indicated in figures corresponds to 1.64×10^4 photons emitted on the surface.

Image processing was made based on grey scale images of tumors. The images in figures shown in this article were further modified by converting emission intensity to specific colors according to a color bar (Fig. 2). Image processing for elimination of background noise induced by high-energy particles was applied with threshold filtering. The average emission intensity in the total region of the tumor was evaluated after subtraction of

[5]To whom correspondence should be addressed. E-mail: noriaki-o@umin.ac.jp

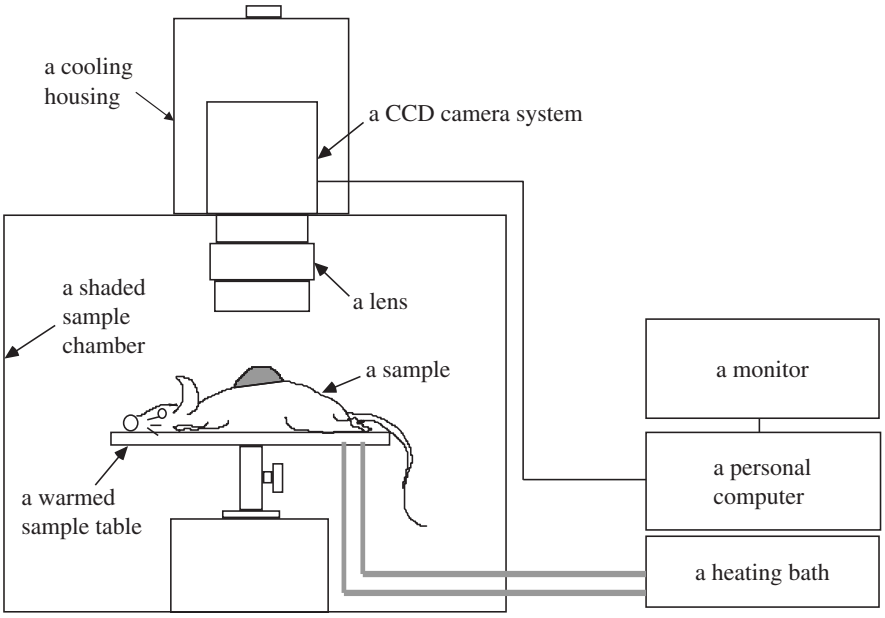

Fig. 1. Schematic of the biophoton imaging system. The biophoton imaging system consists of a liquid nitrogen-cooled highly sensitive CCD camera system (ATC200C, Photometrics), a completely light-shielded sample chamber, a thermostat heater to warm the mice, and a set of computers. The CCD camera system includes a back-illuminated, thinned type Si-CCD (TK1024AB2-G1, Tektronix). The CCD format is 1024×1024 pixels for a full frame, with each pixel size being 24×24 μm. The dark current of the device is 0.225 e^-/h pixel at −120°C in MPP (multipinned phase) mode and the readout noise is 3.3 e^-RMS/pixel.

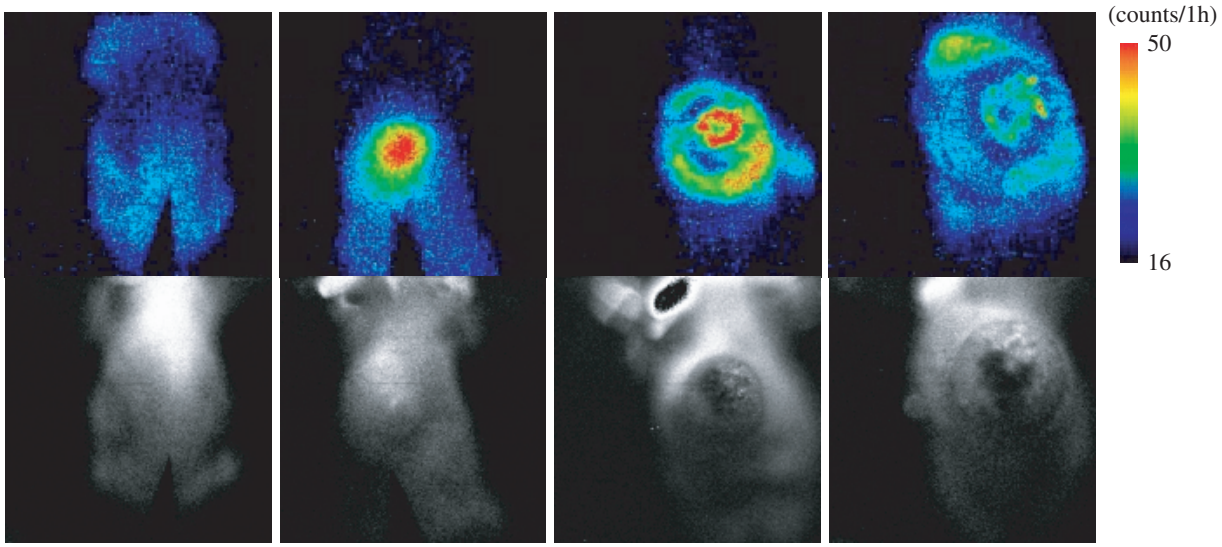

Fig. 2. Biophoton image and pathological findings of AH109A at week 1. The arrows drawn on the tumor corresponds to the cross-sectional line.

the background emission of the mouse determined at a circular region of 600–800 pixels between the blade bones, which exhibited good reproducibility with the lowest biophoton emission in the body of the mice.

Cell lines. The cell lines used in the present study were TE4, TE9 and AH109A. Both TE4 and TE9 are human esophageal carcinoma cell lines established in our department.[13] AH109A is a rat hepatoma cell line.[14] All of the cell lines were cultured in an RPMI1640 medium supplemented with 10% fetal bovine serum. The TE4 and TE9 cells were harvested for transplantation after detachment with trypsin and ethylenediaminetetraacetic acid (EDTA) when the cells were confluent on the bottom of the flasks. The AH109A cells proliferated as a suspension in the medium. The cell suspension was then centrifuged, and cells were collected for transplantation.

Chemicals and animals. We used RPMI1640 medium supplemented with 10% fetal bovine serum (FBS) without phenol red for cell culture. The RPMI1640 medium was purchased from Life Technologies, Inc. (Grand Island, NY) and the FBS was purchased from ICN, Inc. (Costa Mesa, CA). EDTA and trypsin were used to detach the cells from the bottom of the sample cuvettes and culture flasks. The EDTA was purchased from Life Technologies, Inc. and the trypsin was purchased from ICN, Inc. All chemicals were of culture grade.

Mice supplemented in this study were *nu/nu* male nude mice, 5–7 weeks old, purchased from Charles Liver, Inc.

Sample preparation and experimental details. Cells of each line (10^7 cells) were suspended in 0.1 ml of saline (cell volume 0.1

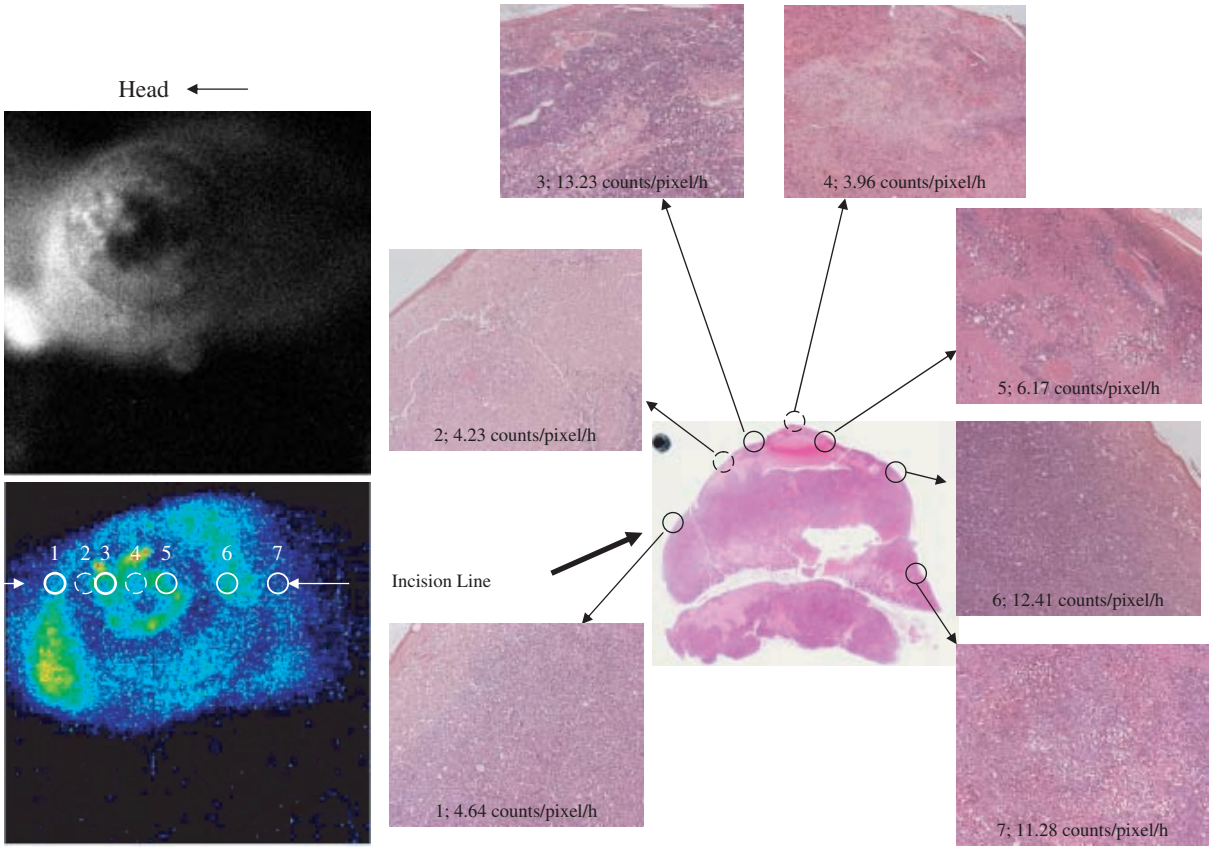

Fig. 3. Changes in the ultraweak biophoton images with tumor growth. Ultraweak biophoton images taken after cell transplantation: week 1, week 2 and week 3.

ml) and 0.2 ml of cell suspension was injected subcutaneously into the backs of the nude mice. After transplantation, the mice were anesthetized with pentobarbital (0.05 mg/g) by intraperitoneal injection and fixed on a temperature-controlled sample table in a completely light-shielded sample chamber. Then biophoton imaging was performed for 1 h with detection of the raw image obtained by a biophoton detector under very weak illumination for estimation of tumor size. Thereafter, the mice were kept in their cages for 1 week and biophoton imaging was performed again for another hour. The correlation between tumor growth rate and biophoton intensity was made at week 1 because AH109A exhibited the fastest growth at that time point; at later times, tumor necrosis appears, and heterogeneity of growth occurs so that the growth rate cannot be properly estimated. Throughout the measurements, the body temperature of the mice was kept at about 37°C.

In some cases the nude mice were kept for 3 weeks for detection of ultraweak biophoton images and pathological examination. After biophoton imaging, the mice were sacrificed by cervical dislocation, and the tumors were excised and embedded in 10% buffered formalin for fixation. We sketched the shape of the tumor mass when we cut the sample for formalin fixation, and we compared the sketch of the pathological sample with the biophoton images. The measurement points of biophoton intensity were carefully identified. Comparison of the biophoton images and pathological slices revealed the relationship between the pathological findings and the two-dimensional biophoton images.

All animal experiments were approved by the Institutional Laboratory Animal Care and Use Committee of Tohoku University. All experiments were performed under UKCCCR guidelines (Workman *et al*., 1998).[15]

Evaluation of growth rate and statistical analysis. Since the same numbers of cells in the same volume of 0.1 ml were introduced at the point of transplantation, we determined the size of tumors at week 1 to calculate the growth rate. The tumor size at week 1 was estimated from the product of the longest diameter and its perpendicular diameter. Tumor height was not measured at week 1 because the tumor was so thin that it was very difficult to measure.

Estimation of the tumor size and the emission intensity of biophoton images at week 1 were performed for 7 TE9 tumors, 9 TE4 tumors and 17 AH109A tumors. The emission intensity was measured by averaging the total tumor area with subtraction of background biophoton intensity obtained from the data measured at the midpoint of bilateral blade bones on the back of mice (this point exhibited the most stable biophoton intensity in the body throughout the measurement period).

The correlation coefficient was calculated from the biophoton intensity and tumor size (area) or square root of tumor size at week 1.

Biophoton intensity and tumor viability. To compare live and necrotic tumor, we observed 5 AH109A xenografts at 3 weeks. We classified each area into live or necrotic tissue, then we measured the biophoton intensity of corresponding circular areas of 697 pixels in biophoton images (Fig. 3). The intensity was measured in 40 live areas and 26 necrotic areas. Statistical analysis was done with a two tailed *t* test.

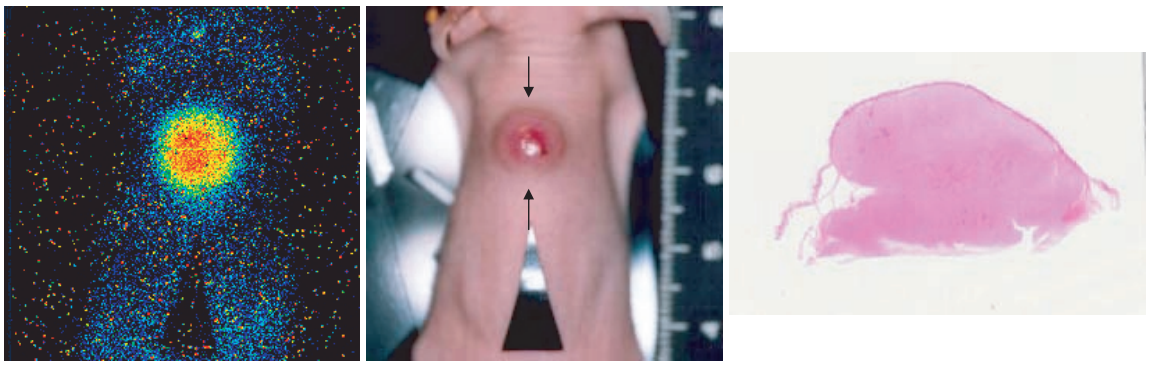

Fig. 4. Comparisons between biophoton image, raw image** and pathological findings of AH109A. An ultraweak biophoton image, raw image and histological images at week 1. The arrows drawn on the tumor corresponds to the cross-sectional line. ** The raw image taken under very weak illumination (3000–5000 photon counts/s) with the CCD camera used for the biophoton imagery.

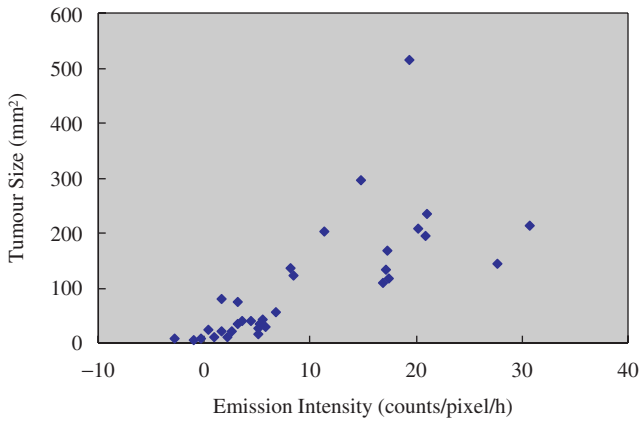

Fig. 5. Correlation between biophoton intensity and square root of tumor size at week 1. Tumor size and ultraweak biophoton intensity at the first week are plotted in the graph. The correlation coefficient of the tumor size at week 1 and ultraweak biophoton intensity is 0.73.

Results

Tumor growth and biophoton imaging. The tumors exhibited different growth modes for each cell line. Representative growth time courses and biophoton images are shown in Fig. 2. The rat hepatoma cell line AH109A showed the most rapid growth, reaching a size of about 700 mm^2 in 3 weeks. The human esophageal carcinoma cell line TE4 grew to the size of about 100 mm^2 in 3 weeks and the human esophageal carcinoma cell line TE9 grew to the size of about 40 mm^2 in a week, but shrank thereafter. The size of TE4 at week 1 was 24 mm^2.

The biophoton patterns also showed differences in each tumor cell strain. Although AH109A exhibited a homogeneous biophoton pattern at week 1, it exhibited a heterogeneous pattern after 2 weeks (Fig. 2). The emission intensity from TE4 was rather weak in the first week, but became more intense in weeks 2 and 3. The biophoton pattern from TE4 showed homogeneity until the third week. In contrast, TE9 showed very weak light emission; tumors were recognized as arising from the lower biophoton intensity area compared to neighboring normal tissue throughout the measurement period.

Nude mice showed specific biophoton emission related to internal organs and muscles in all measurements.

Comparisons of the biophoton pattern and surface appearance of the tumors showed distinct differences. In Fig. 3, part of the tumor showed high-intensity biophoton emission despite being covered with necrotic skin. In another area, the tumor showed low-intensity biophoton emission despite being covered with normal skin. Pathological findings suggest the area with high-intensity biophoton emission contains live tissue and the area with low-intensity biophoton emission contains necrotic tissue (Fig. 3).

Table 1. Comparison of tissue viability and biophoton intensity of AH109A

Tissue viability	Biophoton intensity
Live tissue	2.93±3.34[1)] [2)]
Necrotic tissue	10.76±6.52[1)]

1) Photon counts/pixel/h.
2) *P*=2.30E-8.

Biophoton intensity and tumor growth rate. Pathological observation of AH109A at week 1 revealed homogeneous tissue (Fig. 4).

The average biophoton intensities of the TE9, TE4 and AH109A tumors at week 1 were 3.37±2.23, 2.42±3.09 and 13.55±8.40 counts/pixel/h, respectively. After 1 week, AH109A reached 167.1±55.1 mm^2, while TE9 grew to 41.4±18.7 mm^2 and TE4 grew to 24.1±12.7 mm^2. AH109A showed the highest emission intensity among all the tumors. The biophoton intensity of AH109A was significantly higher than those of TE9 and TE4 (P=0.0001 and P=0.00006, respectively). The P value between TE4 and TE9 was 0.49.

The relationship between biophoton intensity and tumor size at week 1 is shown in Fig. 5. The correlation coefficient of the biophoton intensity and tumor size at week 1 for all tumors was 0.73 and the correlation coefficient of the biophoton intensity and the square root of tumor size was 0.82.

Biophoton intensity and tumor viability. The emission intensity of living tissue, measured in 40 areas, amounted to 10.76±6.52 photon counts/pixel/h, and that of necrotic tissue measured in 26 areas was 2.93±3.34 photon counts/pixel/h. The P value was 0.00077 (Table 1).

Discussion

Although the biophoton images of the AH109A tumor exhibited homogeneous patterns at week 1, they exhibited heterogeneous patterns thereafter. This heterogeneity is not due to the surface condition of the skin, but reflects the viability of the un-

derlying tumor tissue, as judged by microscopic observation.

TE4 grew to approximately 100 mm^2 in 3 weeks and the biophoton image exhibited a homogeneous pattern until the third week. Pathological findings of TE4 showed a homogeneous pattern in accord with the biophoton image.

The biophoton intensity of TE9 at week 1 was greater than that of TE4. TE9 exhibited an extremely weak biophoton intensity at week 3 that was lower than the emission intensity of TE4 or the normal tissue around the tumor. The growth pattern of TE9, i.e., reaching maximum size during week 1 and shrinking thereafter, is in agreement with the biophoton results. Pathological findings showed no vessel formation in TE9.

Although the biophoton images of TE4 and TE9 at week 1 cannot be easily differentiated from those of normal tissue at present, spectral analysis may be helpful for recognition of such tumors.[11)]

The non-tumor regions in the nude mice showed specific biophoton patterns related to the organ distribution. The lumbar muscle and digestive organs showed enhanced biophoton emission. These phenomena suggest that studies to evaluate the relationship between physiological function and biophoton emission would be of value.

The growth rates and biophoton intensities of AH109A tumors are significantly higher than those of TE9 and TE4. Additionally, biophoton intensity and tumor size at week 1 were correlated, with a correlation coefficient of 0.73 (Fig. 5). This result suggests that ultraweak biophoton emission is related to growth activity, presumably via metabolic activity. Thus, we can argue that areas with high intensity of biophoton emission contain live tissue and have high-growth activity, while areas with low-intensity biophoton emission contain necrotic tissue or tissue with a very low-growth rate.

Biophoton emission has been attributed to oxidative metabolism in live organisms, and it was reported that electron leakage from mitochondria results in the generation of active oxygen species such as the superoxide anion, hydrogen peroxide, hydroxyl radical and singlet oxygen.[16)] Oxidation of cellular molecules causes excitement of other fluorescent molecules that results in biophoton emission.[1, 17–19)] In addition, cancer tissue contains fewer reactive oxygen quenchers than normal tissues, including superoxide dismutase (SOD) and catalase.[20)] In normal tissue, reactive oxygen species are immediately eliminated by self-defence mechanisms consisting of SOD, catalase, vitamin E, glutathione, etc., in the cells. In morbid tissue, however, the balance between reactive oxygen generation and quenching activity is destroyed. Although the mechanism of this phenomenon is not clear at present, it is speculated that the relatively fast growth of malignant tumor generates a large amount of reactive oxygen species, leading to intense biophoton emission. The mechanism of this phenomenon should be examined.

Inflammation is also a cause of biophoton emission owing to active oxygen species from neutrophils, which generate singlet oxygen. Since singlet oxygen shows specific absorption at 703 nm, spectral analysis might be useful to distinguish malignant tissue from inflammation.

Tumor growth rate is one of the most important factors that define malignancy. No existing imaging modality except for positron emission tomography (PET) is able to evaluate metabolic activity. Our results suggest that biophoton measurement can detect growth activity, and it requires no isotope-labeled substrates, nor a cyclotron to prepare them, as is needed for PET. Biophoton measurement requires only a completely shielded space and compact detectors, requiring no chemical administration. Thus, biophoton measurement could be useful as a simple non-invasive method to obtain pathological information. PET is preferably used in screening of distant metastases or occult lesions of malignancies. Applications of biophoton measurement should be different from those of PET, because biophoton emission at the body surface represents light emission from only as deep as 3 mm from the tissue surface. Thus, biophoton measurement might be suitable for non-invasive sequential or repeated pathological diagnoses of recognized tumors but not for screening. For measurement of deeper tissue, a needle-coupled measurement probe would be needed. Biophoton measurements also have the advantage of being inexpensive.

This measurement technique may also be available for recognizing extremely thin tumors that are not palpable or visually apparent.

Image aquisition took 1 h in this study, and the measurement time should be shortened for clinical application. Recent development of measurement apparatus with high efficiency can shorten the image acquisition time, which is less than 30 min with the latest detector.

Biophoton images obtained from growing tumors can provide information about tumor properties, including whether the tumor is alive or not and how fast it is growing. In addition, biophoton images reveal tumor viability even when the surface skin is necrotic.

The effectiveness of chemotherapy is generally assessed in terms of tumor size. However, this standard parameter often shows a slow response after application of anticancer therapies, because the reduction of tumor size usually occurs much later than tissue necrosis. Therefore real-time estimation is impossible using this parameter. Biophoton measurements might allow real-time assessment of tumor viability through detection of changes in emission intensity.

In our study, necrotic areas showed low emission intensity in the heterogeneous mass. These results suggest that we can distinguish living area and necrotic area by biophoton measurement. Moreover, sequential measurement of biophoton emission during chemotherapy may enable us to detect tumor necrosis induced by chemotherapy. Because different chemotherapeutic agents have distinct mechanisms of action, characteristic changes of biophoton emission during the transition from the living state of the tumor to the necrotic state might be observable.

In conclusion, this method could be useful to assess not only malignancy, but also the efficacy of chemotherapy or radiotherapy in terms of viability, rather than tumor size. Although biophoton emission can be detected only on the body surface at present, deeper targets should be detected by the use of endoscopy or needle-coupled devices. This procedure may thus provide a non-invasive or minimally invasive optical biopsy as an adjunct to or replacement of existing diagnostic methods. We are now trying to detect other malignant xenografts to confirm the validity of this approach to measure tumor growth rate.

The authors thank Professor Kudo of the Medical Cell Storage Center, Institute of Aging, Tohoku University for providing the TE4, TE9 and AH109A cell lines. The authors declare that they have no competing financial interests.

1. Popp FA, Gurwitsch AA, Inaba H, Slawinski J, Cilento G, van Wijk R, Chwirot WB, Nagl W. Biophoton emission. *Experientia* 1988; **44**: 543–630.
2. Quickenden TI, Que Hee SS. Weak luminescence from the yeast *Saccharomyces cerevisiae* and the existence of mitogenetic radiation. *Biochem Biophys Res Commun* 1974; **60** (2): 764–70.
3. Totsune H, Nakano M, Inaba H. Chemiluminescence from bamboo shoot cut. *Biochem Biophys Res Commun* 1993; **194** (3): 1025–9.
4. Suzuki S, Usa M, Nagoshi T, Kobayashi M, Watanabe H, Inaba H. Two-dimensional imaging and counting of ultraweak emission patterns from injured plant seedlings. *J Photochem Photobiol B Biol* 1991; **9**: 211–7.

5. Takahashi A, Totsune-Nakano H, Nakano M, Mashiko S, Suzuki N, Ohma C, Inaba H. Generation of O_2^- and tyrosine cation-mediated chemiluminescence during the fertilization of sea urchin eggs. *FEBS Lett* 1989; **246**: 117–9.
6. Yoda B, Abe R, Goto Y, Saeki A, Takyu C, Inaba H. Spontaneous chemiluminescence of smoker's blood. In: Kricka LJ, Stanley PE, Thorp GHG, Whitehead TP, editors. Analytical applications of bioluminescence and chemiluminescence. Orlando, FL: Academic Press; 1984. p. 587–90.
7. Gisler GC, Diaz J, Duran N. Observation on blood plasma chemiluminescence in normal subjects and cancer patients. *Arq Biol Technol* 1983; **26** (3): 345–352.
8. Chilton CP, Rose GA. Urinary chemiluminescence-an evaluation of its use in clinical practice. *Br J Urol* 1984; **56**: 650–4.
9. Shimizu Y, Inaba H, Kumaki K, Mizuno K, Hata S, Tomita S. Measuring methods for ultra-low light intensity and their application to extra-weak spontaneous bioluminescence from living tissues. *IEEE Trans Instrum Meas* 1973; **IM-22**: 153–7.
10. Amano T, Kobayashi M, Devaraj B, Usa M, Inaba H. Ultraweak biophoton emission imaging of transplanted bladder cancer. *Urol Res* 1995; **23**: 315–8.
11. Takeda M, Tanno Y, Kobayashi M, Devaraj B, Usa M, Ohuchi N, Inaba H. A novel method of cancer cell proliferation by biophoton emission. *Cancer Lett* 1998; **127**: 155–60.
12. Kobayashi M, Devaraj B, Usa M, Tanno Y, Takeda M, Inaba H. Two-dimensional imaging of ultraweak photon emission from germinating soybean seedlings with a highly sensitive CCD camera. *Photochem Photobiol* 1997; **65** (3): 535–7.
13. Nishihira T, Katayama M, Hashimoto Y, Akaishi T. Cell lines from esophageal tumors. In: Atlas of human tumor cell lines. Academic Press Inc; 1994. p. 269–85.
14. Odashima S. Establishment of ascites hepatoma in the rat, 1951–1963. Ascites tumors-Yoshida sarcoma and ascites hepatoma(s). *Natl Cancer Inst Monogr* 1964; **16**: 51–93.
15. Workman P, Twentyman P, Balkwill F, Balmain A, Chaplin D, Double J, Embleton J, Newell D, Raymond R, Stables J, Stephens T, Wallace J. United Kingdom co-ordinating Committee on Cancer Research (UKCCCR) Guidelines for the welfare of animals in experimental neoplasia (second edition). *Br J Cancer* 1998; **77**: 1–10.
16. Murphy ME, Sies H. Visible-range low-level chemiluminescence in biological systems. *Methods Enzymol* 1990; **186**: 595–610.
17. Cadenas E, Boveris A, Chance B. Low-level chemiluminescence of bovine heart submitochondrial particles. *Biochem J* 1980; **186**: 659–67.
18. Howes RM, Steele RH. Microsomal chemiluminescence induced by NADPH and its relation to lipid peroxidation. *Res Commun Chem Pathol Pharmacol* 1971; **2**: 619–26.
19. Vladimilov Yu A, Roshchupkin DI, Fesenko EE. Photochemical reactions in amino acid residues and inactivation of enzymes during UV irradiation. *Photochem Photobiol* 1970; **11**: 227–46.
20. Oberly LW, Spitz DR. Assay of superoxide dismutase activity in tumor tissue. *Methods Enzymol* 1984; **105**: 457–64.